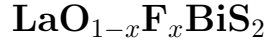


Phonon spectra and superconductivity of BiS₂-based compounds



B. Li and Z. W. Xing*

*National Laboratory of Solid State Microstructures and
Department of Materials Science and Engineering,
Nanjing University, Nanjing 210093, China*

G. Q. Huang

Departement of Physics, Nanjing Normal University, Nanjing 210046, China

Abstract

Using the density-functional perturbation theory with structural optimization, we investigate the electronic structure, phonon spectra, and superconductivity of BiS₂-based layered compounds LaO_{1-x}F_xBiS₂. For LaO_{0.5}F_{0.5}BiS₂, the calculated electron-phonon coupling constant is equal to $\lambda = 0.8$, and obtained $T_c \simeq 9.1$ K is very close to its experimental value, indicating that it is a conventional electron-phonon superconductor.

PACS numbers: 74.20.Pq, 74.25.Kc, 63.20.kd

The recent discovery of superconductivity in the BiS₂-based compounds has attracted much attention due to their layered crystal structure and physical properties similar to cuprate and Fe-based superconductors. The Bi₄O₄S₃ superconductor was found to exhibit metallic transport behavior and to show a zero-resistivity state below 4.5 K.¹ Soon after, another type of BiS₂-based systems, ReO_{1-x}F_xBiS₂ (Re = La, Ce, Pr, and Nd), were reported to be superconducting with transition temperatures T_c equal to 10.6, 3.0, 5.5, and 5.6 K, respectively.²⁻⁵ For Bi₄O₄S₃ (ReO_{1-x}F_xBiS₂), superconductivity can be obtained by electrons doping into the insulating parent compound Bi₆O₈S₅ (ReOBiS₂). Experimental and theoretical studies indicated that these materials exhibit multiband behavior with dominant electron carriers originating mainly from the Bi 6*p* orbitals.^{1,6-12}

In this Letter we report the calculated results for the electronic structure of LaO_{1-x}F_xBiS₂ ($x = 0, 0.5, \text{ and } 1$), phonon dispersions and electron-phonon coupling of superconducting LaO_{0.5}F_{0.5}BiS₂. From the first-principles calculation, it is shown that the parent compound LaOBiS₂ is a band insulator with an energy gap of ~ 0.8 eV, similar to the ground state of cuprate and pnictide superconductors. Upon F doping, the Fermi level moves up and the system appears a metallic nature. We obtain electron-phonon coupling constant $\lambda = 0.8$ and superconducting transition temperature $T_c \simeq 9.1$ K in LaO_{0.5}F_{0.5}BiS₂, indicating that this compound can be explained as a conventional phonon-mediated superconductor, quite different from the Fe-based materials^{13,14} but somewhat similar to the Ni-based compounds.^{15,16}

We used the full-potential linearized augmented plane wave method implemented in the WIEN2K package¹⁷ for the lattice parameter optimization and electronic structure calculations. The generalized gradient approximation (GGA) presented by Wu and Cohen¹⁸ was used for the exchange-correlation energy calculations. This GGA is a nonempirical approximation that gives significant improvements of calculations for lattice constants and crystal structures. The phonon dispersion and the electron-phonon coupling are calculated using density functional perturbation theory (DFPT). The phonon dispersions were obtained in linear response via the QUANTUM-ESPRESSO program¹⁹ and ultrasoft pseudopotentials. The GGA of Perdew-Burke-Ernzerhof²⁰ was adopted for the exchange-correlation potentials with a cutoff of 60 Ry for the wave functions and 600 Ry for the charge density.

LaO_{1-x}F_xBiS₂ with $x=0$ or 1 is crystallized in the ZrCuSiAs type tetragonal structure (P4/nmm) with La, Bi, S1 in the Bi planes, S2 in between Bi-S1 and La-O(F) planes, and

TABLE I: Various optimized structural parameters for $\text{LaO}_{1-x}\text{F}_x\text{BiS}_2$ with $x=0, 0.5$, and 1 .

	LaOBiS ₂	LaO _{0.5} F _{0.5} BiS ₂	LaFBiS ₂
a (Å)	4.0677	4.1091	4.1524
c (Å)	14.3085	13.4196	12.9554
V (Å ³)	236.75	226.59	223.38
z_{La}	0.0890	0.1073	0.1276
z_{Bi}	0.6309	0.6145	0.6090
z_{S1}	0.3945	0.3844	0.3691
z_{S2}	0.8073	0.8128	0.8163
d_{Bi-S1} (Å)	2.8993	2.9056	2.9499
d_{Bi-S2} (Å)	2.5231	2.6621	2.6862

O(F) being at the positions $2c(0.5, 0, z_{La})$, $2c(0.5, 0, z_{Bi})$, $2c(0.5, 0, z_{S1})$, $2c(0.5, 0, z_{S2})$, and $2a(0, 0, 0)$, respectively. The F substitution at the O sites in $\text{LaO}_{0.5}\text{F}_{0.5}\text{BiS}_2$ reduces the symmetry to a space group of P-4m2. Starting from the lattice parameters ($a = 4.0527$ Å and $c = 13.3237$ Å) reported by Mizuguchi *et al.*², we have performed the full structural optimization including the lattice parameters and atomic positions, the obtained results being summarized in Table I. It is found that, with doping F from $x = 0$ to $x = 1$, the a value increases gradually but the c value decreases, accompanied with a decrease of primitive cell volume V . By making a comparison in the atomic bond length between $\text{LaO}_{0.5}\text{F}_{0.5}\text{BiS}_2$ and LaOBiS_2 , one finds that the Bi-S2 bond expands due to F doping while d_{Bi-S1} for the Bi-S1 bond remains almost unchanged.

The calculated band structures and electronic density of states (DOS) are shown in Fig. 1. The contribution of orbital states to the band structure are characterized by different colors: blue (Bi- p), red (S1- p), and green (O- p and S2- p). For LaOBiS_2 , the Fermi level is located at the upper edge of valence bands with an energy gap of ~ 0.8 eV, indicating an insulating behavior. The valence bands spread from around -6 eV to 0 and consist of the p states of the O and S atoms. While the La- d and La- f states lie above 4 eV, far away from the Fermi level, the Bi- p and S1- p states dominate the conduction bands. For doped $\text{LaO}_{0.5}\text{F}_{0.5}\text{BiS}_2$, the Fermi level enters the conduction bands coming from the Bi- p

TABLE II: Phonon mode frequencies (cm^{-1}) at Γ and M points in $\text{LaO}_{0.5}\text{F}_{0.5}\text{BiS}_2$. I: infrared active, R: Raman active.

$\Gamma(0, 0, 0)$						
$B_2(I+R)$	0	65.4	145.4	249.4	270.1	412.2
$E(I+R)$	0	39.3	44.0	78.4	122.8	
		153.6	171.3	184.1	243.8	345.1
$A_1(R)$	74.8	138.3	168.4	305.9		
$M(0.5, 0.5, 0)$						
A_1	61.3	81.3	155.8	195.8		
A_2	55.5	101.7	123.5	189.3	275.8	
B_1	60.8	81.6	169.5	199.6		
B_2	56.3	94.3	103.3	191.0	299.6	
E	71.0	74.9	148.4	220.5	269.8	403.4

and S1- p states, so that the Bi-S1 layers dominantly contribute to the electronic conduction. As shown in Fig. 1b, the present Fermi level crosses four bands of electron pockets, and so $\text{LaO}_{0.5}\text{F}_{0.5}\text{BiS}_2$ has electron carriers, which is well consistent with the Hall resistance measurements.¹⁰ The DOS at the Fermi level is equal to $N(E_F) = 1.22 \text{ eV}^{-1}$ on a per formula unit both spins basis, and the corresponding bare susceptibility and specific heat coefficient are given by $\chi_0 = 4.0 \times 10^{-5} \text{ emu/mol}$ and $\gamma_0 = 3.0 \text{ mJ/mol K}^2$, respectively. For LaFBiS_2 , the Fermi level further enters the conduction bands and the energy gap increases to $\sim 1.1 \text{ eV}$. Meanwhile, the DOS at the Fermi level increases to $N(E_F) = 1.84 \text{ eV}^{-1}$ per formula unit both spins, yielding $\chi_0 = 6.0 \times 10^{-5} \text{ emu/mol}$ and $\gamma_0 = 4.5 \text{ mJ/mol K}^2$.

The calculated phonon dispersions of $\text{LaO}_{0.5}\text{F}_{0.5}\text{BiS}_2$ are plotted in Fig. 2a, in which there are 30 phonon bands extending up to $\sim 450 \text{ cm}^{-1}$ and the point group at the Γ and M points is D_{2d} . The Γ and M -point modes can be decomposed as $\Gamma = 6B_2 \oplus 10E \oplus 4A_1$ and $M = 4B_1 \oplus 4A_1 \oplus 5B_2 \oplus 5A_2 \oplus 6E$. Note that the E mode is degenerate, and its frequencies are listed in Table II. The Raman modes at the zone center can be measured directly by experiments in near future. The corresponding phonon density of states (PDOS), Eliashberg spectral function $\alpha^2F(\omega)$, electron-phonon coupling $\lambda(\omega)$ and projected PDOS

are shown in Fig. 3. There are three distinct peaks centered at $\sim 70 \text{ cm}^{-1}$ (A_1 mode at Γ point), $\sim 190 \text{ cm}^{-1}$ (E mode at Γ point), and $\sim 250 \text{ cm}^{-1}$ (B_2 mode at Γ point), respectively, corresponding to three thick lines from lower to upper in Fig. 2a. As shown in Fig. 2b, the A_1 mode corresponds to the vertical vibrations with the upper and lower BiS_2 -layers (La-layers) beating against each other. The E mode corresponds to the in-plane stretching vibrations with motion along the $x(y)$ axis. In the B_2 mode, the La, Bi, and S1 atoms vibrate along the same z direction, opposite to the vibration direction of the S2, O, and F atoms. From Fig. 3, one can see that the bands around 70 cm^{-1} comes mainly from the PDOS contributions of the Bi and La motion, the peak at 190 cm^{-1} mainly corresponds to the S character, and that at 250 cm^{-1} corresponds to F, O and S character. The calculated Eliashberg spectral function has peaks in consistent with the PDOS at the low-frequency regime, and is evidently enhanced in the intermediate frequency regime. In the DFPT calculations, the Eliashberg spectral function depends directly on the electron-phonon matrix element:

$$\alpha^2 F(\omega) = \frac{1}{N(E_F)N_k} \sum_{kq\nu} |g_{n\mathbf{k},m(\mathbf{k}+\mathbf{q})}^\nu|^2 \times \delta(\varepsilon_{n\mathbf{k}})\delta(\varepsilon_{m(\mathbf{k}+\mathbf{q})})\delta(\omega - \omega_{q\nu}). \quad (1)$$

Here, N_k is the number of \mathbf{k} points used in the summation, $N(E_F)$ is the density of states at the Fermi level, and $\omega_{q\nu}$ are the phonon frequencies. The electron-phonon matrix element $|g_{n\mathbf{k},m(\mathbf{k}+\mathbf{q})}^\nu|^2$ is defined by the variation in the self-consistent crystal potential. It follows that the electron-phonon interaction of Bi-S1 bond plays an important role in the enhancement of $\alpha^2 F(\omega)$. From the $\lambda(\omega)$ curves in Fig. 3a, where $\lambda(\omega) = 2 \int_0^\omega [\alpha^2 F(\Omega)/\Omega] d\Omega$, one finds that $\lambda(220) \simeq 0.7$ has been close to $\lambda(\infty) \simeq 0.8$, indicating that the phonon modes in the low and intermediate frequency regimes have the main contribution to the electron-phonon coupling. From the $\alpha^2 F(\omega)$ spectra in Fig. 3, we get the electron-phonon coupling $\lambda = 0.8$ and the logarithmically averaged frequency $\omega_{ln} = 192 \text{ K}$. Using further the Allen-Dynes formula with the Coulomb parameter $\mu^* = 0.1$, we finally obtain $T_c = 9.1 \text{ K}$, which is found very close to the experimental value $T_c = 10.6 \text{ K}$.² It then follows that the doped $\text{LaO}_{0.5}\text{F}_{0.5}\text{BiS}_2$ is very likely a conventional electron-phonon superconductor.

In summary, the present first-principles calculations indicate that $\text{LaO}_{1-x}\text{F}_x\text{BiS}_2$ changes from a band insulator at $x = 0$ to a band metal upon doping. Similar to $\text{LaFeAsO}_{1-x}\text{F}_x$, electrons in $\text{LaO}_{1-x}\text{F}_x\text{BiS}_2$ are doped from the LaO(F) redox layer to the superconducting BiS_2 layers. The p -orbital states of Bi-S1 layers play an important role in the electron

transformation due to their domination of the DOS at the Fermi level. From the phonon calculations for $\text{LaO}_{0.5}\text{F}_{0.5}\text{BiS}_2$, we obtain a strong electron-phonon coupling of $\lambda = 0.8$ and a superconducting transition temperature of $T_c = 9.1$ K, the latter being very close to its experimental value. It then follows that $\text{LaO}_{0.5}\text{F}_{0.5}\text{BiS}_2$ is a conventional electron-phonon superconductor.

For $\text{LaO}_{1-x}\text{F}_x\text{BiS}_2$, we have shown that the electronic states near the Fermi level are dominantly from the hybridized p orbital states of the Bi and S1 atoms, and the electron-phonon coupling comes mainly from the contribution of the Bi and S phonons. These facts indicate that the BiS_2 layers play an important role in the transport and superconducting properties, similar to the CuO_2 layers of the cuprates or Fe-As layers of the Fe-based superconductors.

I. ACKNOWLEDGMENTS

This work is supported by the State Key Program for Basic Researches of China (2010CB923404), the National Natural Science Foundation of China (11074109 and 11174125), the National "Climbing" Program of China (91021003), and the Natural Science Foundation of Jiangsu Province (BK2010012).

* Electronic address: zwxing@nju.edu.cn

¹ MIZUGUCHI Y., FUJIHISA H., GOTOH Y., SUZUKI K., USUI H., KUROKI K., DEMURA S., TAKANO Y., IZAWA H., and MIURA O., arXiv:1207.3145 (2012).

² MIZUGUCHI Y., DEMURA S., DEGUCHI K., TAKANO Y., FUJIHISA H., GOTOH Y., IZAWA H., and MIURA O., arXiv:1207.3558 (2012).

³ XING J., LI S., DING X., YANG H., and WEN H.-H., arXiv:1208.5000 (2012).

⁴ JHA R., SINGH S. K., and AWANA V. P. S., arXiv:1208.5873 (2012).

⁵ DEMURA S., MIZUGUCHI Y., DEGUCHI K., OKAZAKI H., HARA H., WATANABE T., DENHOLME S. J., FUJIOKA M., OZAKI T., FUJIHISA H., GOTOH Y., MIURA O., YAMAGUCHI T., TAKEYA H., and TAKANO Y., arXiv:1207.5248 (2012).

⁶ USUI H., SUZUKI K., and KUROKI K., arXiv:1207.3888 (2012).

- ⁷ LI S., YANG H., TAO J., DING X., and WEN H.-H., arXiv:1207.4955 (2012).
- ⁸ SINGH S. K., KUMAR A., GAHTORI B., SHRUTI, SHARMA G., PATNAIK S., and AWANA V. P. S., arXiv:1207.5428 (2012).
- ⁹ TAN S. G., LI L. J., LIU Y., TONG P., ZHAO B. C., LU W. J., and SUN Y. P., arXiv:1207.5395 (2012).
- ¹⁰ AWANA V. P. S., KUMAR A., JHA R., KUMAR S., KUMAR J., PAL A., SHRUTI, SAHA J., and PATNAIK S., arXiv:1207.6845 (2012).
- ¹¹ WAN X. G., DING H. C., SAVRASOV S., DUAN C. G., arXiv:1208.1807v2 (2012).
- ¹² YILDIRIM T., arXiv:1210.2418v1 (2012).
- ¹³ BOERI L., DOLGOV O. V., and GOLUBOV A. A., *Phys.Rev.Lett.*, **101** (2008) 026403.
- ¹⁴ LI B., XING Z. W., and LIU M., *Appl.Phys.Lett.* **98** (2011) 072506; LI B., XING Z. W., HUANG G. Q., and M. Liu, *J.Appl.Phys.*, **111** (2012) 033922.
- ¹⁵ SUBEDI A., SINGH D. J. and DU M.-H., *Phys.Rev.B*, **78** (2008) 060506(R).
- ¹⁶ SUBEDI A., and SINGH D. J., *Phys.Rev.B*, **78** (2008) 132511(R).
- ¹⁷ BLAHA P., SCHWARZ K., MADSEN G., KVASNICKA D., and LUITZ J., *WIEN2K* (Technische Universitat Wien, Austria, 2007).
- ¹⁸ WU Z., and COHEN R. E., *Phys.Rev.B*, **73** (2006) 235116.
- ¹⁹ See <http://www.quantum-espresso.org> for information about QUANTUM-ESPRESSO code.
- ²⁰ PERDEW J. P., BURKE K., and ERNZERHOF M., *Phys.Rev.Lett.*, **77** (1996) 3865.

Figure Caption

Figure 1. (Color online) Calculated band structure and density of states of $\text{LaO}_{1-x}\text{F}_x\text{BiS}_2$ for $x=0$ (a), 0.5 (b), and 1 (c), with orbital character indicated by different colors: Bi- p (blue), S1- p (red), and O- p and S2- p (green).

Figure 2. (Color online) (a) Calculated phonon dispersion curves of $\text{LaO}_{0.5}\text{F}_{0.5}\text{BiS}_2$. (b) Atom vibration pattern of the A_1 , E and B_2 modes at Γ point.

Figure 3. (Color online) (a) Phonon density of states $G(\omega)$, electron-phonon spectral function $\alpha^2F(\omega)$ and electron-phonon coupling $\lambda(\omega)$ for $\text{LaO}_{0.5}\text{F}_{0.5}\text{BiS}_2$. (b) Projected phonon density of states for each atom.

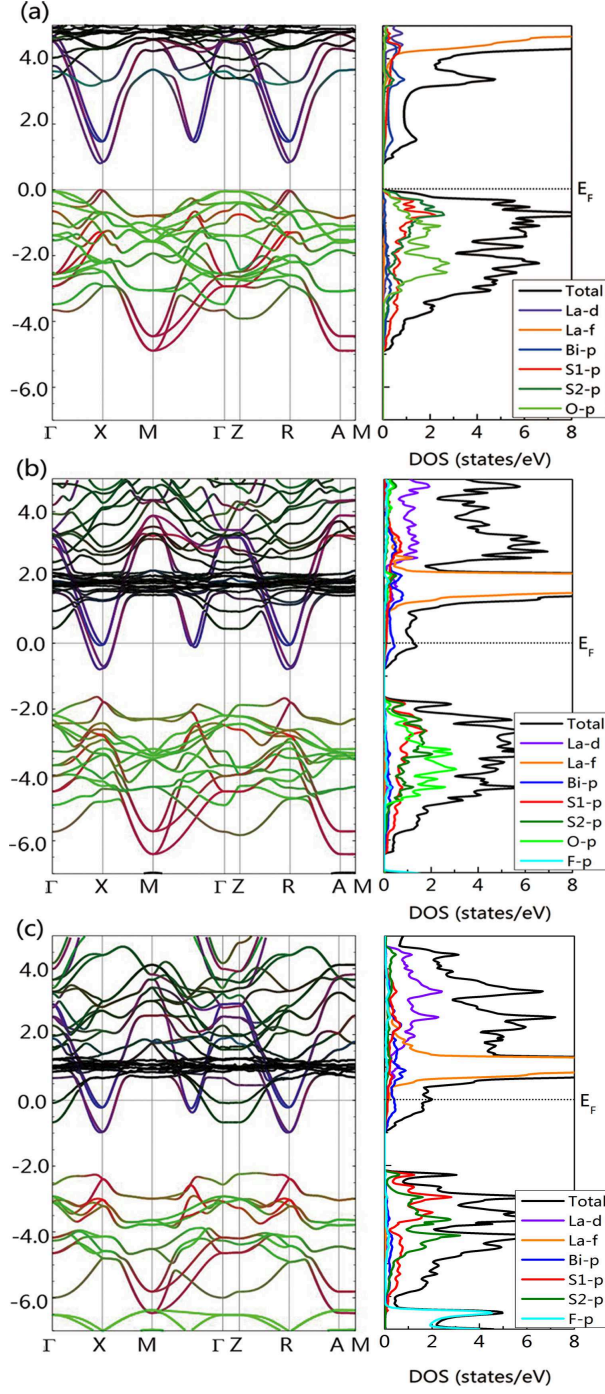


FIG. 1: Calculated band structure and density of states for $\text{LaO}_{1-x}\text{F}_x\text{BiS}_2$ with $x=0$ (a), 0.5 (b), and 1 (c) with orbital character indicated by different colors: Bi- p (blue), S1- p (red), and O- p and S2- p (green).

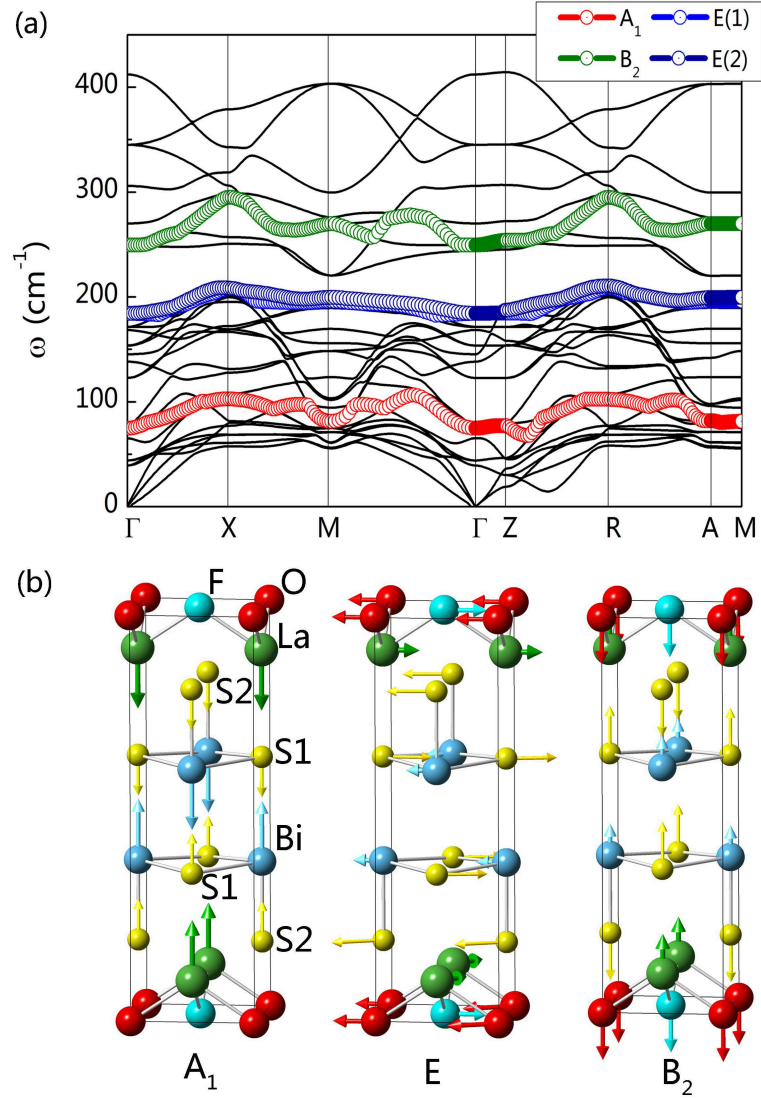


FIG. 2: (a) Calculated phonon dispersion curves of $\text{LaO}_{0.5}\text{F}_{0.5}\text{BiS}_2$. (b) Atom vibration pattern of the A_1 , E and B_2 modes at Γ point.

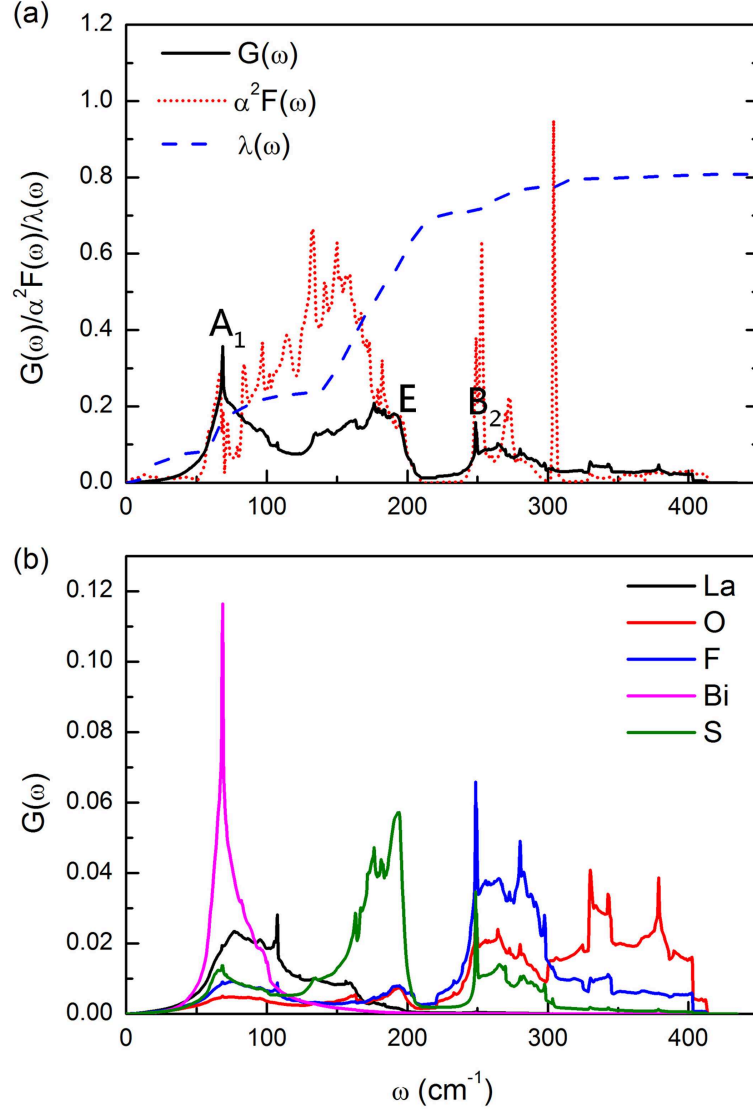


FIG. 3: (a) Phonon density of states $G(\omega)$, electron-phonon spectral function $\alpha^2 F(\omega)$ and electron-phonon coupling $\lambda(\omega)$ for $\text{LaO}_{0.5}\text{F}_{0.5}\text{BiS}_2$. (b) Projected phonon density of states for each atom.